MOOSE Project Part 3

Hongsup Oh

1 Introduction

In MOOSE Project Part 3, we need to implement a swelling model that incorporates thermal expansion, densification, and fission product-induced swelling. Additionally, we are required to present the updated results from Part 1 and Part 2. The model uses the same domain as in Part 1—the fuel pellet has a radius of 0.5 cm, the gap is 0.005 cm thick, the cladding is 0.1 cm thick, and all components have a height of 1 cm. However, in this part, the focus is on analyzing the thermo-mechanical behavior of the fuel system. The project report focuses on presenting the results from MOOSE and is structured into five sections: MOOSE Project Part 1, MOOSE Project Part2 , and MOOSE Project Part 3.

2 MOOSE Project Part 1

2.1 Steady state problem with constant k

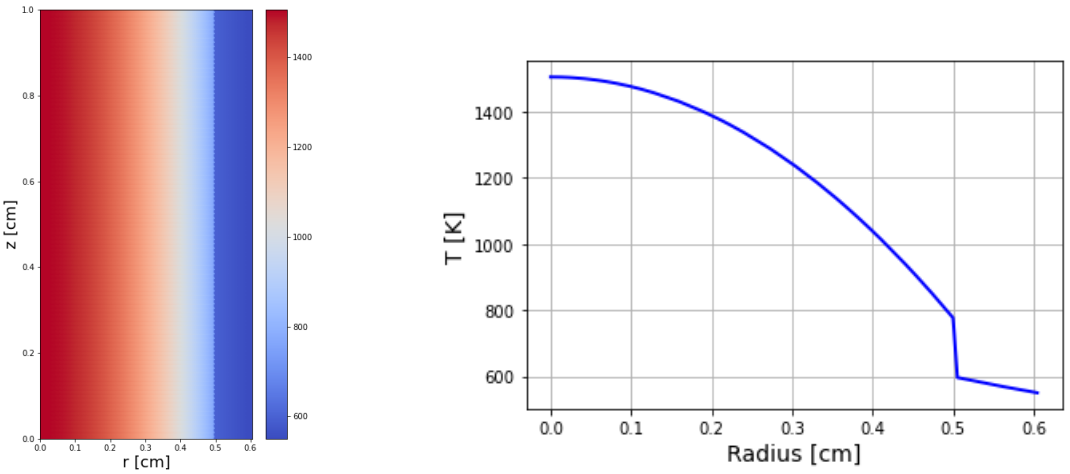

(a) Temperature distribution in the fuel system

(b) Temperature profile in the fuel system

Figure 1: The result of steady state problem with constant k

The input and output files for this section are **project1_steady.i** and **project1_steady_out.e**. Figure 1 presents the results of the steady-state problem with a constant thermal conductivity. Figure 1a illustrates the overall temperature distribution within the fuel domain, while Figure 1b shows the corresponding temperature profile. The fuel pellet is assumed to be UO2 with a thermal conductivity of 0.03 W/cm·K, the gap is filled with helium with a thermal conductivity of 0.00256 W/cm·K, and the cladding is modeled as Zircaloy with a thermal conductivity of 0.17 W/cm·K.

2.2 Steady state problem with temperature dependent k

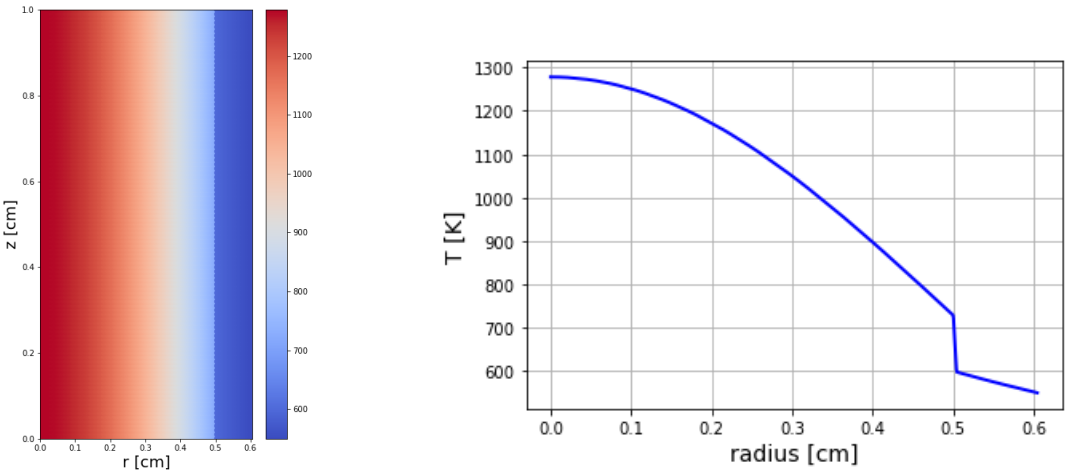

(a) Temperature distribution in the fuel system

(b) Temperature profile in the fuel system

Figure 2: The result of steady state problem with constant k

The input and output files for this section are **project1_steady_k_temp_dependent.i** and **project1_steady_k_temp_dependent_out.e**. Figure 2 presents the results of the steady-state problem with temperature dependent thermal conductivity. Figure 2a illustrates the overall temperature distribution within the fuel domain, while Figure 2b shows the corresponding temperature profile. The fuel pellet is assumed to be UO2, with its thermal conductivity defined as:

$$k_p(T) = \frac{1}{3.8 + 0.0217 \cdot T} \quad [W/cm - K] \tag{1}$$

Equation **??** is taken from the lecture notes (Lecture 4, page 15). The gap between the pellet and cladding is assumed to be filled with helium (He), and its thermal conductivity is given by:

$$k_g(T) = (4.68e-4) + (3.81e-6) \cdot T - (6.79e-10) \cdot T^2 \quad [W/cm - K] \tag{2}$$

Lastly, the cladding material is assumed to be zirconium (Zr), with its thermal conductivity expressed as:

$$k_c(T) = (0.1098) + (1.4e-4) \cdot T - (7.44e-8) \cdot T^2 \quad [W/cm - K] \tag{3}$$

Equations 2 and 3 are taken from Newman, Hansen, and Gaston (2008) [2]. The centerline temperature decreases compared to the case with constant thermal conductivity, but the difference is not significant.

2.3 Transient problem with constant k

The input and output files for this section are **project1_transient.i** and **project1_transient_out.e**. The linear heat rate (LHR) is defined as a time-dependent function:

$$LHR(t) = 350 \left(\exp\left(-\frac{(t-20)^2}{2} \right) + 1 \right) \quad [W/cm] \tag{4}$$

Figure 3 shows the results of the transient problem with constant thermal conductivity. Figure 3a illustrates the overall temperature distribution within the fuel domain after reaching steady state, while Figure 3b depicts the evolution of the maximum temperature over time steps. The thermal

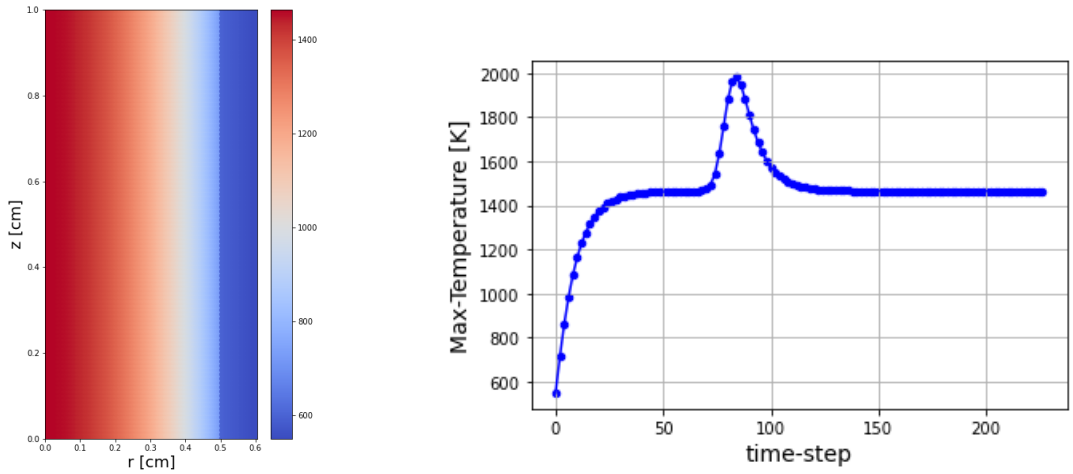

(a) Temperature distribution in the fuel system (b) The evolution of maximum temperature over time-steps

Figure 3: The result of transient problem with constant k

conductivities used are the same as those in Section 2.1. Figure 3b shows the maximum temperature at each time step. The temperature rises until around time step 70, experiences a significant jump near step 80, and then gradually decreases before stabilizing.

2.4 Transient problem with temperature dependent k

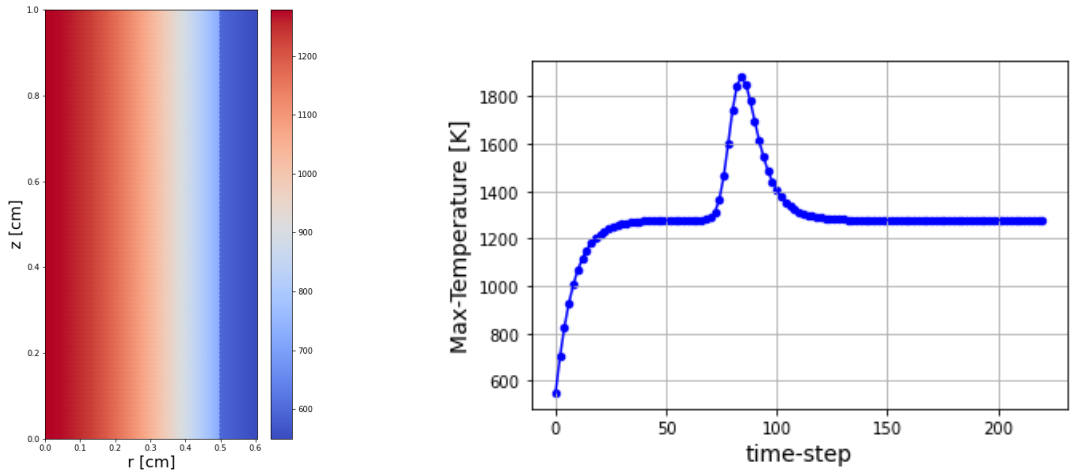

(a) Temperature distribution in the fuel system (b) The evolution of maximum temperature over time-steps

Figure 4: The result of transient problem with temperature dependent k

The input and output files for this section are **project1_transient_k_temperature_dependent.i** and **project1_transient_k_temperature_dependent_out.e**. A time-dependent linear heat rate (LHR), defined by Equation 4, is used in this analysis. Figure 4 shows the results of the transient prob-

lem with temperature dependent thermal conductivity. Figure 4a illustrates the overall temperature distribution within the fuel domain after reaching steady state, while Figure 4b depicts the evolution of the maximum temperature over time steps. The thermal conductivities of the fuel pellet, gap, and cladding are given by Equations 1 to 3. The maximum temperature profile is similar to the case with constant thermal conductivity, but the overall temperature is lower.

3 MOOSE Project Part 2

The input and output files for this section are **project2_transient.i** and **project2_transient_out.e**. In MOOSE Project Part 2, the equations for LHR and T_{inf}, as well as the values for $\dot{m}$ and C_{PW}, have been updated to match those provided in the lecture notes (Lecture 3, pages 39–41). The axial distribution of LHR is given by the following equation:

$$LHR(z) = LHR_0 \cdot \cos\left(\frac{\pi}{2\gamma}\left(\frac{z}{z_0} - 1\right)\right) \quad [W/cm] \tag{5}$$

where $LHR_0 = 350$ $[W/cm]$, $z_0 = H/2$ and $\gamma = 1.3$. The axial distribution of T_∞ is given by the following equation:

$$T_\infty(z) = T_\infty(0) + \frac{1}{1.2}\frac{z_0 \cdot LHR_0}{\dot{m}C_{pw}}\left(\sin(1.2) + \sin\left(1.2\left(\frac{z}{z_0} - 1\right)\right)\right) \quad [K] \tag{6}$$

where $T_\infty(0) = 500$ $[K]$, $\dot{m} = 0.25$ $[kg/s - rod]$, and $C_{PW} = 4200$ $[J/kg - K]$. The convective heat transfer coefficient, h_c, is calculated as follows: First, the total flow area is given by:

$$A_x = \left(S^2 - \frac{\pi \cdot D_{co}^2}{4}\right) = (1.2 \cdot 1.21)^2 - \frac{\pi \cdot 1.21^2}{4} = 0.9584 \quad [cm^2]$$

The wetted perimeter is:

$$P_w = \pi \cdot D_{co} = \pi \cdot 1.21 = 3.8013 \quad [cm]$$

The hydraulic diameter is calculated as:

$$D_h = \frac{4 \cdot A_x}{P_w} = \frac{4 \cdot 0.9584}{3.8013} = 1.008493 \quad [cm]$$

To compute the Nusselt number, we first determine the Reynolds and Prandtl numbers:

$$Re = \frac{\dot{m} \cdot D_h}{A_x \cdot \mu} = \frac{0.25 \cdot 1.008493}{0.9584 \cdot 8.9e-4} = 295.58$$

Prandtl number (Pr) is:

$$Pr = \frac{C_{pw} \cdot \mu}{k} = \frac{4200 \cdot 8.9e-4}{0.606} = 6.1683$$

The Nusselt number is then estimated using an empirical correlation:

$$Nu = \left(0.042\frac{S}{D_{co}} - 0.024\right) Re^{0.8} Pr^{0.33} = \left(0.042\frac{1.2 \cdot 1.21}{1.21} - 0.024\right) 295.58^{0.8} 6.1683^{0.33} = 4.5593$$

Finally, the convective heat transfer coefficient (h_c) is:

$$h_c = \frac{Nu \cdot k}{D_h} = \frac{4.5593 \cdot 0.606}{1.008493} = 2.7396 \quad [W/cm^2 - K] \tag{7}$$

The value obtained from Equation 7 is close to the value provided in the lecture notes, which was 2.6 $[W/cm^2 - K]$. Figure 5 presents the results of Project 2. Figure 5a illustrates the overall tem-

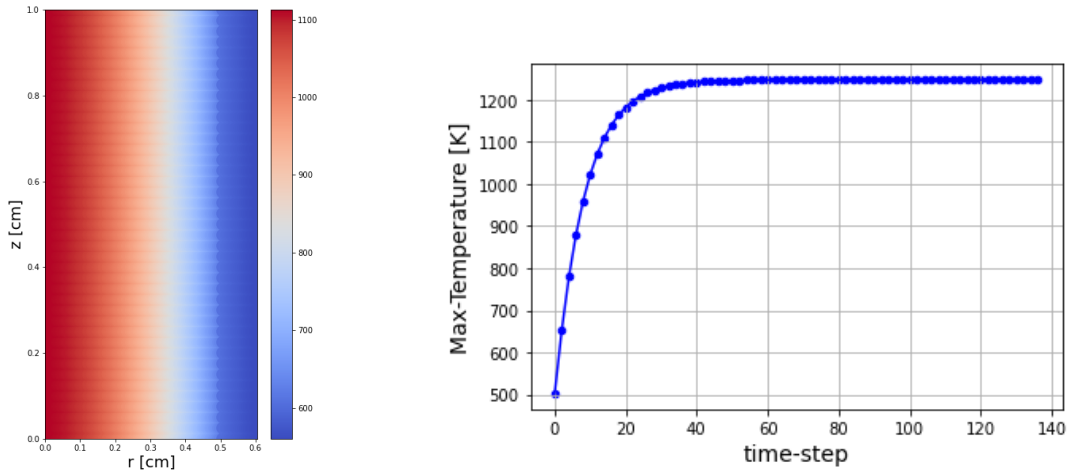

(a) Temperature distribution in the fuel system (b) The evolution of maximum temperature over time-steps

Figure 5: The result of transient problem with time dependent LHR and T_∞

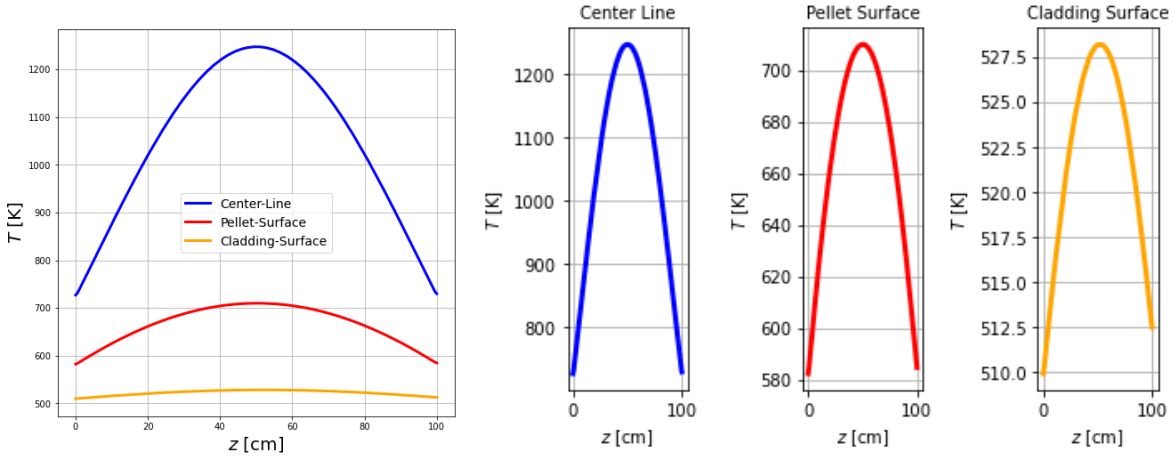

(a) One plot for three temperature profiles. (b) Separated plots for three temperature profiles.

Figure 6: Temperature profile for fuel center line (blue), pellet surface (red), and cladding surface (orange).

perature distribution in the fuel, reflecting the sinusoidal nature of the applied function. Figure **??** shows the evolution of the maximum temperature over time, which increases in a parabolic manner before converging around 1300 K. Figure 6 shows the temperature profiles at the fuel centerline, pellet surface, and cladding surface. The overall trend is consistent with the results from the Project 2 report, although the temperature values are slightly lower across the board. Asymmetry in the profile is evident at the cladding surface, and slight differences in temperature can also be observed at both ends of the pellet surface and centerline.

4 MOOSE Project Part 3

4.1 Eqillibrium Equation

The input and output files for this section are **project3_input.i** and **project3_input_out.e**. In MOOSE Project Part 3, we analyze the effects of fuel swelling induced by thermal expansion, densification, and fission product accumulation. This project requires solving a coupled thermomechanical problem, involving both heat transfer and solid mechanics. The mechanical equilibrium equation is given by:

$$\nabla \cdot \boldsymbol{\sigma} + f = 0 \tag{8}$$

The constitutive relation for the stress tensor is:

$$\boldsymbol{\sigma} = \mathbb{C} : \boldsymbol{\varepsilon}_{TOT} \tag{9}$$

where the total strain $\boldsymbol{\varepsilon}_{tot}$ includes contributions from multiple sources:

$$\varepsilon_{TOT} = \varepsilon_T + \varepsilon_D + \varepsilon_{SFP} + \varepsilon_{GFP}$$

Here, the subscripts T, D, SFP, and GFP represent thermal strain, densification strain, solid fission product swelling, and gaseous fission product swelling, respectively.

4.2 Strain Components & Material Properties

First, the thermal strain is defined by the following equation:

$$\varepsilon_t = \alpha \left(T - T_{ref}\right) \tag{10}$$

Thermal strain is applied to all materials in the system, including the fuel pellet, gap, and cladding. The reference temperature T_{ref} represents the stress-free temperature—i.e., the temperature at which no thermal stress is generated. In this project, the reference temperature is set to $T_{ref} = 300$. The coefficients of thermal expansion are assigned as follows: $\alpha_p = 12e-6$ $[1/K]$ for the fuel pellet, $\alpha_g = 0.0$ $[1/K]$ for the gap, and $\alpha_c = 7e-6$ $[1/K]$ for the cladding. Second, the densification strain is defined by the following equation:

$$\varepsilon_D = \Delta\rho_0 \left(\exp\left(\frac{\beta \ln 0.01}{C_D \beta_D}\right) - 1\right) \tag{11}$$

where β is burnup [FIMA], $\Delta\rho_0 = 0.01$ is total densification that can occur, $\beta_D = 0.005$ [FIMA] is burnup at which densification stops, and $C_D = 7.235 - 0.0086\,(T - 298.15)$ [K] for $T < 1023.15$ [K] and $C_D = 1$ for $T \geq 1023.15$ [K]. Densification strain is only applied to the fuel pellet. Third, the solid fission product strain is defined by the following equation:

$$\varepsilon_{SFP} = (5.577e-2)\rho\beta \tag{12}$$

where β [FIMA] represents the burnup, and $\rho = 10.98$ $[g/cm^3]$ is the density of the fuel pellet. The solid fission product strain is applied exclusively to the fuel pellet. Fourth, the strain of the gaseous fission product is defined by the following equation:

$$\varepsilon_{GFP} = (1.96e-28)\rho\beta(2800 - T)^{11.73} \exp(-0.0162(2800 - T)) \exp(-17.8\rho\beta) \tag{13}$$

The gaseous fission product strain is applied only to the fuel pellet. This strain is applied exclusively to the fuel pellet. For simplification, we consider only the strain in the x-direction. As a result, the total strain tensor is represented as:

$$\boldsymbol{\varepsilon}_{TOT} = \begin{bmatrix} \varepsilon_{TOT} & 0 & 0 \\ 0 & 0 & 0 \\ 0 & 0 & 0 \end{bmatrix} \tag{14}$$

Table 1: Material properties of the fuel system

Material	UO2	He	Zr
E [GPa]	20	0.0	8
ν	0.345	0.0	0.41

Material properties required for the analysis, such as Young's modulus and Poisson's ratio, are summarized in Table 1. The gap is modeled as a vacuum with thermal conductivity. However, assigning a zero value for Young's modulus causes errors in MOOSE, so a small nonzero value (e.g., 1e-6) is used instead.

4.3 Burnup

In Project 3, we account for the effects of burnup on the fuel system. The first step is to calculate the fission rate using the following equation:

$$\dot{F} = \frac{\dot{q}}{\alpha} = \frac{LHR}{A \cdot \alpha} = \frac{350}{(\pi \cdot 0.5^2) \cdot (3.28451e-11)} = 1.356e+13 \quad [fission/m^3/s] \tag{15}$$

Here, $\dot{q}$ $[W/m^3]$ is the volumetric heat generation rate, A is the cross-sectional area of the fuel pellet, and α [J/fission] is the energy released per fission. The next step is to calculate the number of moles of UO2 in the fuel sample [1]:

$$N_{UO2} = \frac{\rho N_{av}}{M_{UO2}} = \frac{10.48 \cdot (6.022e+23)}{270.03} = 2.337e+22 \quad [atoms/cm^2] \tag{16}$$

Finally, the burnup, expressed in FIMA (Fissions per Initial Metal Atom), is calculated as:

$$\beta = \frac{\dot{F} \cdot t}{N_{UO2}} = \frac{(1.356e+13) \cdot t}{2.337e+22} = (5.8052e-10) \cdot t \quad [FIMA] \tag{17}$$

4.4 Temperature Dependent Thermal Conductivity

Thermal conductivity of gap and cladding are Equation 2 and 3 respectively. For the fuel pellet, the thermal conductivity as a function of temperature T and burnup β is given by:

$$k_p(T, \beta) = \frac{1}{3.8 + 200 \cdot \beta + 0.0217 \cdot T} \quad [W/cm - K] \tag{18}$$

4.5 Results

In reality, the gap is nearly closed but not entirely, as mesh elements still occupy the gap region. This near-closure can lead to convergence issues during simulation. To address this, a coarser mesh is employed compared to Projects 1 and 2, with 110 nodes in the x-direction and 40 nodes in the y-direction. For simplification, zero Dirichlet boundary conditions are applied to the top, bottom, and right surfaces of the fuel system.

To solve the thermo-mechanical problem, the `SolidMechanics` kernel is additionally required in this project. Since there are no externally applied forces causing displacement, only eigenstrains need to be considered. For thermally induced strain, a built-in function is available. However, other sources of strain—such as densification, solid fission product swelling, and gaseous fission product swelling—do not have built-in models. These additional eigenstrains are implemented in the `Materials` block using `ParsedMaterial` and `ComputeVariableEigenstrain` functions. Each resulting eigenstrain field is stored using `AuxVariable` and extracted via `AuxKernel`. The simulation was terminated at step

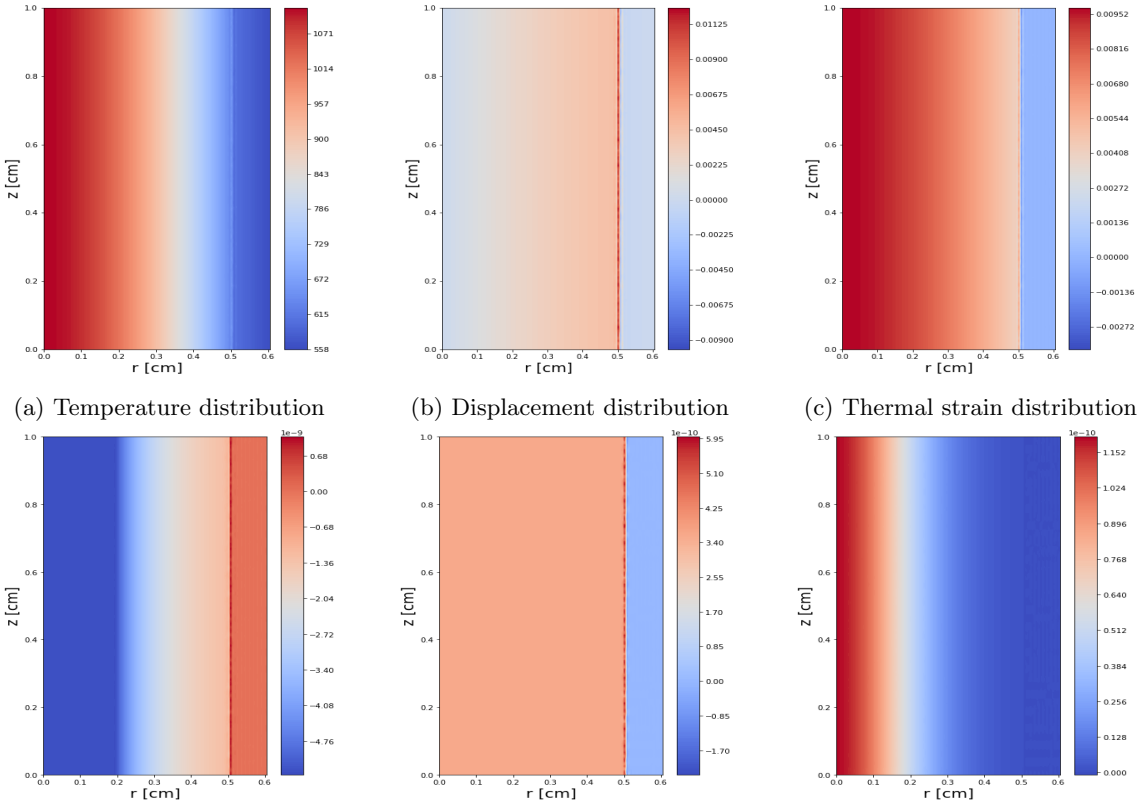

(a) Temperature distribution (b) Displacement distribution (c) Thermal strain distribution

(d) Densification strain distribution (e) SFP strain distribution (f) GFP strain distribution

Figure 7: Result of Project 3

248 (time = 7.6) due to a convergence issue. The results from the final step—including temperature, x-displacement, thermal strain, densification strain, solid fission product (SFP) strain, and gaseous fission product (GFP) strain—are presented in Figure 7. Figure 8 summarizes the time evolution of maximum temperature, displacement, and strains from Figure 8a to Figure 8f. Thermal strain (Figure 8c) and GFP strain (Figure 8f) increase over time, while SFP strain (Figure 8e) remains positive and nearly constant. Densification strain (Figure 8d) is negative and decreases with time. Overall, the simulation results align well with the theoretical principles presented in the lecture. Finally, the results of gap closure are presented. The empty space in Figure 9a illustrates the initial gap, which is 0.05 cm. Figure 9b shows the final gap state, reduced to approximately 0.006 cm.

5 Conclusion

In MOOSE Project 3, a thermo-mechanical problem is addressed. The simulation analyzes the temperature evolution within the fuel system, along with swelling contributions from thermal expansion, densification, solid fission products, and gaseous fission products. Among these mechanisms, thermal expansion is the primary contributor to overall swelling, while densification is the only process resulting in shrinkage. Due to the inclusion of mesh elements in the gap region, the simulation requires significant computational time to fully capture gap closure. In this study, the gap was not observed to completely close, but it was nearly closed by the end of the simulation. It is expected that continued simulation would result in further gap closure.

Additionally, the results of Projects 1 and 2 are briefly revisited based on received feedback. For

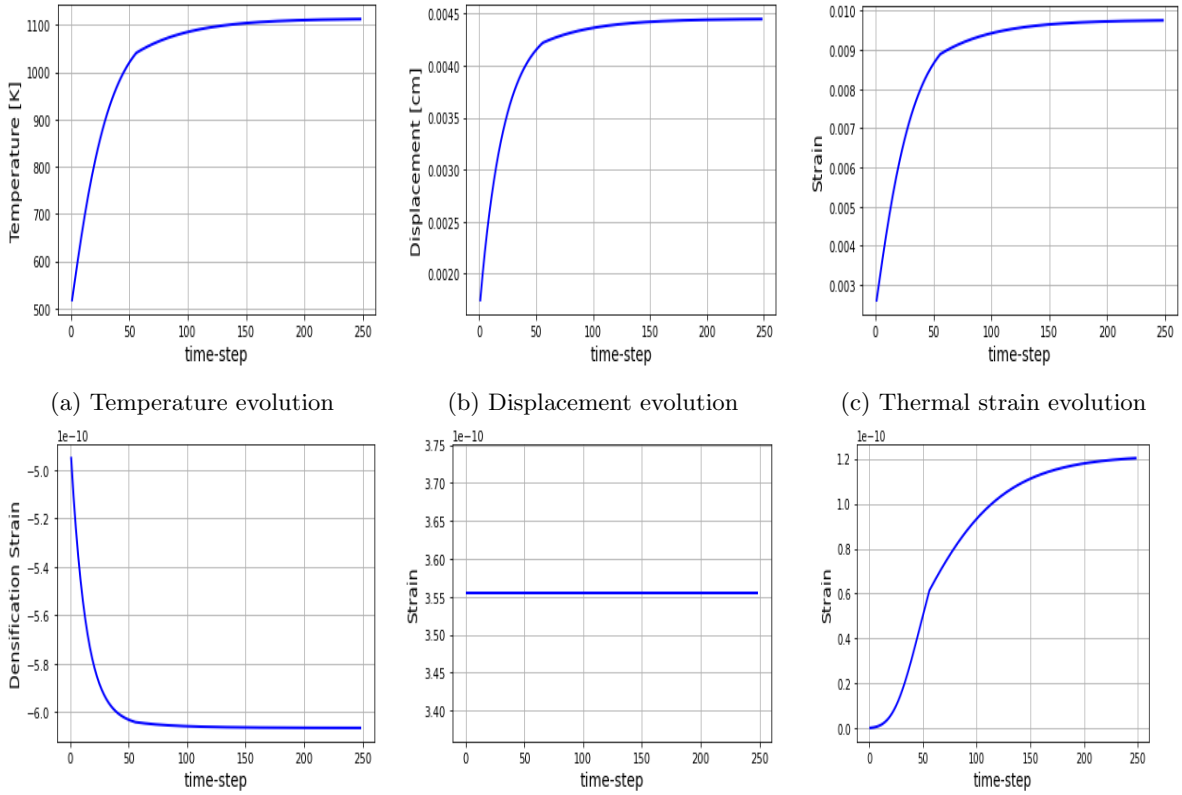

(a) Temperature evolution (b) Displacement evolution (c) Thermal strain evolution

(d) Densification strain evolution (e) SFP strain evolution (f) GFP strain evolution

Figure 8: Result of Project 3 over time-steps

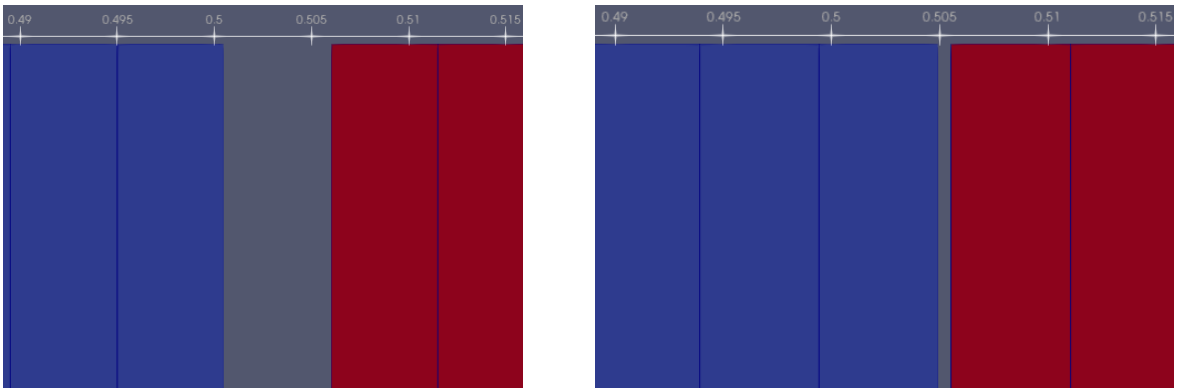

(a) The initial gap condition (b) Final gap state

Figure 9: Gap Closure Results

Project 1, the previously observed fluctuation issue has been resolved, and convergence problems have also been addressed. In Project 2, the linear heat rate (LHR) and ambient temperature T_∞ were updated to match the values provided in the lecture notes. The method for calculating the convective heat transfer coefficient h_c was corrected, resulting in a value that closely matches the one introduced in the lecture. While the results remain consistent with those from the original Project 2 report, the

overall temperature is slightly lower. As future work, I plan to revise Project 3 based on upcoming feedback.

References

[1] Idaho National Laboratory. Bison: Nuclear fuel performance code, 2011.

[2] Chris Newman, Glen Hansen, and Derek Gaston. Three dimensional coupled simulation of thermomechanics, heat, and oxygen diffusion in uo2 nuclear fuel rods. *Journal of Nuclear Materials*, 392(1):6–15, 2009.